NRC Publications Archive
Archives des publications du CNRC

Kinetics of the addition of olefins to Si-centered radicals: The critical role of dispersion interactions revealed by theory and experiment
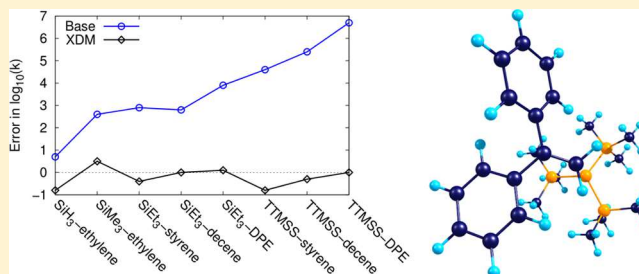Johnson, Erin R.; Clarkin, Owen J.; Dale, Stephen G.; Dilabio, Gino A.

Kinetics of the Addition of Olefins to Si-Centered Radicals: The Critical Role of Dispersion Interactions Revealed by Theory and Experiment

Erin R. Johnson,*[†,¶] Owen J. Clarkin,[‡] Stephen G. Dale,[¶] and Gino A. DiLabio*[§,⊥]

[†]Department of Chemistry, Dalhousie University, 6274 Coburg Road, Halifax, Nova Scotia, Canada B3H 4R2

[‡]University of Ottawa Heart Institute, 40 Ruskin Street, Ottawa, Ontario, Canada K1Y 4W7

[¶]Chemistry and Chemical Biology, University of California, Merced, 5200 North Lake Road, Merced, California 95343, United States

[§]Department of Chemistry, University of British Columbia, Okanagan, 3247 University Way, Kelowna, British Columbia, Canada V1V 1V7

[⊥]National Institute for Nanotechnology, National Research Council of Canada, 11421 Saskatchewan Drive, Edmonton, Alberta, Canada T6G 2M9

S *Supporting Information*

ABSTRACT: Solution-phase rate constants for the addition of selected olefins to the triethylsilyl and tris(trimethylsilyl)-silyl radicals are measured using laser-flash photolysis and competition kinetics. The results are compared with predictions from density functional theory (DFT) calculations, both with and without dispersion corrections obtained from the exchange-hole dipole moment (XDM) model. Without a dispersion correction, the rate constants are consistently underestimated; the errors increase with system size, up to 10^6 s^{-1} for the largest system considered. Dispersion interactions preferentially stabilize the transition states relative to the separated reactants and bring the DFT-calculated rate constants into excellent agreement with experiment. Thus, dispersion interactions are found to play a key role in determining the kinetics for addition reactions, particularly those involving sterically bulky functional groups.

In the past decade, the accurate treatment of noncovalent interactions, particularly dispersion, has risen to the forefront of research in theoretical chemistry. Conventional density functional theory (DFT) methods do not include dispersion physics, and this shortcoming inspired the development of a variety of dispersion-corrected functionals. The inclusion of dispersion is essential to model van der Waals complexes,[1] including guest–host complexes,[2] and for interactions between molecules and surfaces.[3] The effects of dispersion in transition-metal complexes with bulky ligands may even exceed the electrostatic repulsion between metal cations.[4]

Dispersion interactions play an important role in the determination of reaction barrier heights.[5−7] The effects of dispersion will be pronounced in the calculation of bimolecular addition reactions involving large molecules wherein long-range attractive dispersion interactions will stabilize transition states relative to separated reactants and thereby increase the calculated reaction rate constants. In this work, we present a side-by-side comparison of rate constants calculated by dispersion-corrected DFT and experimental kinetics data for a set of bimolecular addition reactions. Pseudo-first-order rate constants for the addition of olefins to silicon-centered radicals are compared to computational rate constant predictions made using DFT methods with and without the inclusion of

dispersion corrections. The results demonstrate that dispersion is essential for the accurate determination of rate constants for bimolecular addition reactions involving even fairly small chemical species.

Silicon-centered radicals are useful reducing agents for organic synthesis and polymerization[8] and also represent a good model for silicon surface reactive sites. Olefin addition to radical sites on otherwise hydrogen-terminated silicon surfaces is the initial step in the formation of linear molecular nanostructures on silicon.[9,10] The work in ref 9 showed that small, straight-chain alkenes could not "grow" molecular lines on silicon, but stryene formed nanostructures quite easily. This supported the hypothesis that the styrene–silicon addition intermediate was stabilized by delocalization of the unpaired spin over the aromatic moiety. It was later convincingly demonstrated that if the dispersion interactions between the incoming molecule and the surface provide sufficient stabilization, alkenes could also be made to form linear nanostructures.[11]

Solution-phase olefin additions to silicon-centered radicals involve chemistry that is similar to that seen on the silicon surface. Their reaction kinetics can be measured using laser-flash photolysis techniques, allowing for a direct comparison of the rate constants with computational predictions. In this work, we performed laser-flash photolysis and competition kinetics,[12] following the work of Chatgilialoglu et al.,[13−15] to measure the rate constants for addition of 1-hexene, 1-decene, 1-pentadecene, styrene, and 1,1-diphenylethylene (DPE) to the triethylsilyl (SiEt$_3$) and tris(trimethylsilyl)silyl (TTMSS) radicals.

The chemistry studied herein can be understood by considering the reactions involving DPE. Di-*tert*-butyl peroxide and DPE were dissolved in isooctance along with either TTMSS or SiEt$_3$. A 308 nm laser was used to homolytically cleave the peroxide O−O bond, resulting in the formation of *tert*-butoxyl (*t*BuO$^\bullet$) radicals. *t*BuO$^\bullet$ then quickly abstracted a hydrogen atom from the Si−H bond of the silane to generate a silicon-centered radical. The Si-centered radicals then reacted with DPE by adding to the terminal CH$_2$ group of the olefin, as shown in Figure 1, to form a Si−C bond and, consequently, a
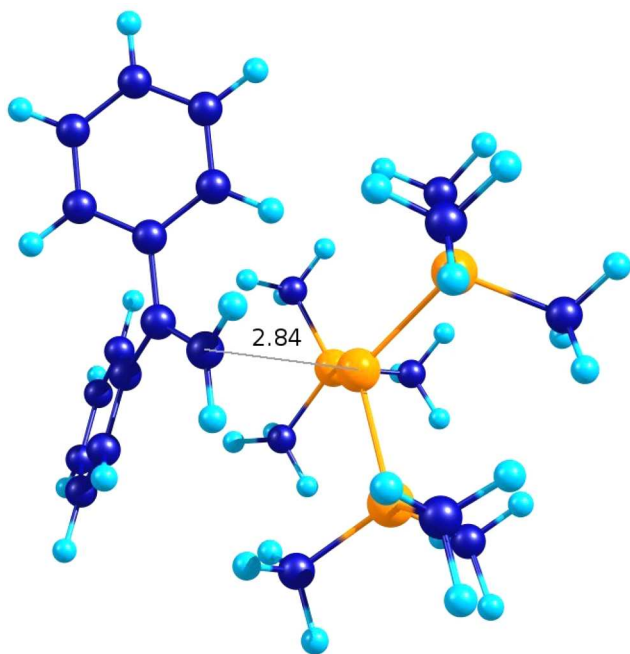

Figure 1. Calculated transition-state structure for addition of DPE to the TTMSS using the LC-ωPBE-XDM//pc-2-spd level of theory. The perspective shows DPE "beside" the TTMSS radical, and the computed key Si−C distance is 2.84 Å. Carbon atoms are represented in dark blue, hydrogen in light blue, and silicon in orange.

carbon-centered radical. The resulting adduct strongly absorbed light in the range of 320−360 nm. The rate of addition of the silyl radical to DPE could then be measured by the change in optical density of the solution as a function of time, assuming that the changes in solution optical density are due entirely to the silyl-DPE adduct.

The rate of addition of the silicon radical to DPE was measured by varying its concentration systematically while holding constant the concentrations of all other species. Since the addition reaction is first-order in DPE, the observed rate constant, k_{obs}, is

$$k_{obs} = k_{DPE}[DPE] + k_0 \tag{1}$$

where k_{DPE} is the rate constant for the addition of the silyl radical to DPE, [DPE] is the concentration, and k_0 is the lifetime of the silyl radical in the absence of DPE. The dependence of the observed rate on initial DPE concentration is shown in Figure 2 for addition to both SiEt$_3$ and TTMSS radicals. The slopes give the pseudo-first-order rate constants for these reactions.
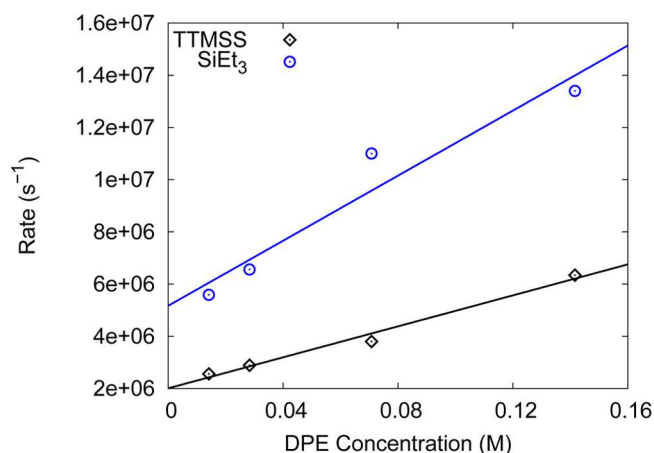

Figure 2. Dependence of observed reaction rate on diphenylethylene concentration for reaction with either SiEt$_3$ or TTMSS radicals, demonstrating pseudo-first-order kinetics.

This reaction of silicon-centered radicals with DPE was also used as a kinetically competitive probe to indirectly measure the rate constants for the addition of silyl radicals to other olefins that do not give a sufficiently strong optical adsorption for direct measurements. When another olefin is present in solution, in addition to DPE, the observed rate constant becomes

$$k_{obs} = k_{DPE}[DPE] + k_{olefin}[olefin] + k_0 \tag{2}$$

If the concentration of DPE is held constant and only the concentration of the other olefin is varied, this simplifies to

$$k_{obs} = k_{olefin}[olefin] + C \tag{3}$$

and this allows for the measurement of the rate constants for addition to styrene, 1-hexene, 1-decene, and 1-pentadecene by competition kinetics. The rate constants so measured[12] are listed in Table 1. The uncertainties of the linear fits are 10% or ±0.1 log units for each rate constant measured. Given the small number of data points, the experimental error bars are expected to be somewhat larger; however, even assuming errors of up to a factor of 2, the uncertainties would be ±0.3 log units or less.

The rate constants for the addition reactions described above were also predicted theoretically using conventional transition-state theory. For the general bimolecular addition reaction

$$A + B \rightarrow TS \rightarrow Products \tag{4}$$

the rate constant, k, is

$$k = \frac{k_B T}{h} \frac{Q_{TS}}{Q_A Q_B} \exp\left(-\frac{\Delta E_0}{RT}\right) \tag{5}$$

where k_B is Boltzmann's constant, h is Planck's constant, R is the gas constant, T is the temperature, the Q's are the partition functions, and ΔE_0 is the zero-point-corrected energy change

Table 1. Comparison of Experimental and Calculated Rate Constants Using Base and XDM-Corrected Functionals[a]

reaction	expt.	XDM-corrected		base functional	
		BH&HLYP	LC-ωPBE	BH&HLYP	LC-ωPBE
CH$_3$−ethylene	2.9[b]	2.7	2.7	1.8	1.7
CH$_3$−propylene	2.7[b]	2.2	2.2	1.2	1.1
CH$_3$−butylene	2.7[b]	2.2	2.2	1.1	1.1
CH$_3$−isobutylene	3.1[b]	2.8	2.8	1.6	1.5
tBu−ethylene	1.5[b]	2.1	2.7	−0.9	0.2
SiH$_3$−ethylene	6.3[c]	7.1	6.9	5.6	5.6
SiMe$_3$−ethylene	6.6[d]	6.1	6.5	4.0	4.4
Si(Et)$_3$−hexene	5.9[e]	5.9	6.9	3.0	3.5
Si(Et)$_3$−decene	6.0[e]	6.0	6.9	3.2	3.6
Si(Et)$_3$−pentadecene	6.3[e]	5.3	6.9	2.9	3.5
Si(Et)$_3$−styrene	7.3[e]	7.7	8.3	4.4	5.5
Si(Et)$_3$−DPE	7.8[e]	7.7	9.3	3.9	5.1
TTMSS−hexene	5.5[e]	5.8	6.5	0.3	1.3
TTMSS−decene	5.6[e]	5.9	6.5	0.2	1.2
TTMSS−pentadecene	5.7[e]	4.9	6.6	0.5	1.1
TTMSS−styrene	7.5[e]	8.3	8.9	2.9	3.7
TTMSS−DPE	7.5[e]	7.5	10.0	0.8	1.7
MAE		0.4	0.9	3.2	2.7
ME		0.0	0.7	−3.2	−2.7

[a]Values are represented as $\log_{10}(k)$. The mean absolute error (MAE) and the mean error (ME) for each method are also shown. Sources of experimental data are. [b]Reference 45. [c]Reference 46. [d]Reference 47. [e]Reference 12 and this work.

between the reactants (A, B) and transition state (TS). The electronic energies, zero-point energy corrections, and partition functions were all computed using DFT methods.

As we will demonstrate, dispersion interactions are critical to obtaining a proper description of the structures and energetics of the transition states for the reactions under study. In this work, we used the exchange-hole dipole moment (XDM) dispersion model of Becke and Johnson.[16,17] The XDM dispersion energy is added as a post-SCF correction to the energy of the base functional

$$E = E_{\text{DFT}} + E_{\text{disp}} \qquad (6)$$

The dispersion energy expression involves a summation over all pairs of atoms i and j and is given by

$$E_{\text{disp}} = -\sum_{n=6,8,10} \sum_{i<j} \frac{C_{n,ij}}{R_{ij}^n + R_{\text{vdW},ij}^n} \qquad (7)$$

In this equation, the dispersion coefficients C_6, C_8, and C_{10} are calculated nonempirically from functions of the electron density and are therefore sensitive to changes in atomic environment. The van der Waals radii, $R_{\text{vdW},ij}$, in the denominator serve to damp the dispersion energy at small interatomic separations, R_{ij}, and involve two (atom-independent) empirical parameters fit for use with a particular base density functional.[17]

For studies of transition states, many-electron self-interaction error in the base functional may have a large effect on the calculated barriers. This error arises because most common density functional approximations fail to give energies that are piecewise linear as a function of electron number and result in the overstabilization of fractional charges.[18−24] The error, which is also referred to as delocalization error, causes band gaps to be underestimated, charge-transfer complexes to be overly stabilized, and electronic transition energies to be underestimated.[25−29] Of particular relevence to this work, the overstabilization of delocalized electron distributions[30−35] results in the underestimation of the barrier heights of radical

reactions. For this study, BH&HLYP[36,37] and LC-ωPBE[38,39] were chosen as the base functionals because they have minimal inherent self-interaction error.[40]

The calculated dissociation energies for bonds between C and Si are known to be quite insensitive to the choice of basis set.[41] However, the accurate treatment of noncovalent interactions requires diffuse basis functions.[42] We therefore chose to use the 6-31+G* basis set with the BH&HLYP functional. For the LC-ωPBE calculations, we used the pc-2-spd basis set (the pc-2 set of Jensen et al.[43,44] with the f functions removed), which also contains diffuse functions, and this method and basis set combination was found to provide the best balance between computational cost and accuracy for intermolecular interactions.[42] To ensure that our electronic energy barrier heights are well converged with respect to basis set size, test calculations were performed on the SiMe$_3$−ethylene complex using the aug-cc-pVTZ basis set. The differences between the XDM-corrected barriers were found to be 0.03 kcal/mol with both BH&HLYP and LC-ωPBE.

The structures for the reactants and transition states of all of the olefin addition reactions were optimized with and without XDM dispersion, using Gaussian 09[48] and the postg program.[17] As an example, the transition state for addition of DPE to TTMSS optimized with LC-ωPBE-XDM is shown in Figure 1. For 1-hexene, 1-decene, and 1-pentadecene, multiple configurations of the alkane chains are possible, but only the straight-chain conformation was studied to simplify the theoretical treatment. It is reasonable to expect that the variability in chain conformations of the isolated alkene will be mirrored by conformations of the chains in the transition-state structure. Consequently, the effect of multiple chain configurations on computed rate constants are expected to cancel.

The absence of rotational symmetry in the SiEt$_3$ radical will result in the formation of several possible low-energy conformers for transition-state complexes in which it is a constituent. To properly calculate rate constants for these cases,

the rate constants associated with each transition-state structure were summed to give the overall rate constant.

The partition functions were computed using the standard rigid rotor and harmonic oscillator approximations. The XDM dispersion correction is also included in calculation of the vibrational frequencies but causes only minor changes in the partition functions and consequently in the pre-exponential factor of the rate constant equation.

Solvent effects were not included in our calculations because we expect the differential effects of hydrocarbon solvent on the separated reactant and the transition-state complexes to be close to zero. To support this expectation, a test calculation was performed on the $SiMe_3$–ethylene system using a polarizable continuum model[49] of isooctane solvent (2,2,4-trimethylpentane in Gaussian 09[48] with a dielectric constant of 1.9358). The calculation resulted in an increase in the reaction barrier of only 0.2 kcal/mol.

The measured and calculated rate constants for all of the olefin additions to $SiEt_3$ and TTMSS are collected in Table 1. Also included are calculated results for the addition of small olefins to methyl, *tert*-butyl, and silyl radicals, where dispersion is expected to have a smaller effect due to the smaller molecular size. Experimental rate constants for these additional reactions were taken from literature sources.[45−47] All of the rate constants are expressed as $\log_{10}(k)$. The mean error (ME) and mean absolute error (MAE) in the rate constants are reported and are also expressed in logarithmic units. For example, a ME of one log unit indicates that the method overestimates the rate constants by 1 order of magnitude on average.

The results in Table 1 show that the base functionals, without dispersion corrections, predict rate constants that are in reasonable agreement with the measured values only for the smallest reactants, namely, CH_3–ethylene and SiH_3–ethylene. Of course, rate constants are exponentially dependent on barrier heights, and even for these small systems, the rate constant is underestimated by up to an order of magnitude. The underestimation reflects calculated barriers that are too high to the extent that 1 order of magnitude error in rate constant is equivalent to a 1.3 kcal/mol error in reaction barrier. Overestimated barriers indicate the pathological tendency for nondispersion-corrected DFT methods to be overly repulsive at van der Waals distances. As the molecular size of the reactants increases, so too does the extent of underestimation of the calculated rate constant, as shown in Figure 3. The monotonic underestimation of the calculated rate constant with increasing size reaches more than 6 orders of magnitude for the largest system studied in this work.

The inclusion of dispersion reduces addition barriers by differentially stabilizing the transition-state complexes relative to the reactants. For example, for the H–ethylene addition barrier, dispersion contributes 0.3 kcal/mol. As the systems increase in size, the increasing differential dispersion stabilization of the transition states ranges from just over 1 kcal/mol for CH_3–ethylene to as much as 10 kcal/mol for TTMSS–DPE. With the XDM dispersion corrections included, both the BH&HLYP and LC-ωPBE functionals predict the rate constants to within less than an order of magnitude of the experimental values on average. The only large outlier is TTMSS–DPE with LC-ωPBE-XDM, which overbinds the transition state and overestimates the rate constant. The rate constant for $SiEt_3$–DPE is also overestimated with LC-ωPBE-XDM, and these errors are likely due to the known sensitivity
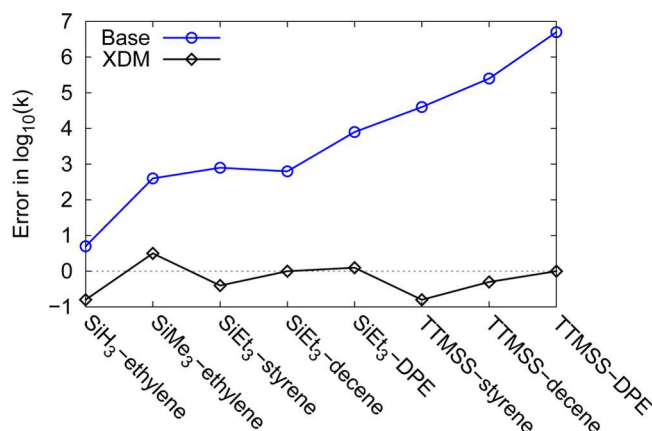

Figure 3. Errors in the computed BH&HLYP rate constants with (XDM) and without XDM dispersion (Base) as a function of increasing reactant size.

of this class of functional (range-separated hybrids) to the extent of conjugation.[50] However, BH&HLYP-XDM provides good agreement with experiment for complexes involving DPE and gives the lowest MAE of the two DFT-based methods considered, of only 0.4 for $\log(k)$; this indicates that the predicted rate constants agree with experiment to within a factor of 2.5 on average.

In summary, by comparing theoretical and experimental results for rate constants of a set of olefin addition reactions, we find that dispersion plays a major role in stabilizing the transition state. In the absence of dispersion, rate constants for addition to TTMSS are predicted to be smaller than those for addition to $SiEt_3$ due to the greater steric bulk of TTMSS. However, the inclusion of dispersion results in greater calculated relative stabilization of the transition-state complexes relative to reactants for the reactions involving TTMSS, decreasing the activation energy and increasing the rate constant. Thus, dispersion interactions play a key role in the thermodynamics and kinetics of addition reactions, particularly for sterically bulky molecules or surfaces. Dispersion interactions should therefore be included in the DFT modeling of all chemical systems.

■ ASSOCIATED CONTENT

⊛ Supporting Information

Transition-state geometries and details of the laser flash photolysis experiments. The Supporting Information is available free of charge on the ACS Publications website at DOI: 10.1021/acs.jpca.5b03251.

■ AUTHOR INFORMATION

Corresponding Authors

*E-mail: erin.johnson@dal.ca (E.R.J.).
*E-mail: gino.dilabio@ubc.ca (G.A.D.).

Notes

The authors declare no competing financial interest.

■ ACKNOWLEDGMENTS

■ REFERENCES

(1) DiLabio, G. A., Otero-de-la Roza, A. Dispersion Interactions in Density-Functional Theory *Rev. Comput. Chem.* **2014**arXiv:1405.1771.

(2) Risthaus, T.; Grimme, S. Benchmarking of London Dispersion-Accounting Density Functional Theory Methods on Very Large Molecular Complexes. *J. Chem. Theory Comput.* **2013**, *9*, 1580−1591.

(3) Ye, Z.; Otero-de-la Roza, A.; Johnson, E. R.; Martini, A. Effect of Tip Shape on Atomic-Friction at Graphite Step Edges. *Appl. Phys. Lett.* **2013**, *103*, 081601.

(4) Grimme, S.; Djukic, J.-P. Cation−Cation Attraction: When London Dispersion Attraction Wins over Coulomb Repulsion. *Inorg. Chem.* **2011**, *50*, 2619−2628.

(5) Mazzonna, M.; Bietti, M.; DiLabio, G. A.; Lanzalunga, O.; Salamone, M. Importance of π-Stacking Interactions in the Hydrogen Atom Transfer Reactions from Activated Phenols to Short-Lived *n*-Oxyl Radicals. *J. Org. Chem.* **2014**, *79*, 5209−5218.

(6) D'Alfonso, C.; Bietti, M.; DiLabio, G. A.; Lanzalunga, O.; Salamone, M. Reactions of the Phthalimide *n*-Oxyl Radical (PINO) with Activated Phenols: The Contribution of π-Stacking Interactions to Hydrogen Atom Transfer Rates. *J. Org. Chem.* **2013**, *78*, 1026−1037.

(7) Bietti, M.; DiLabio, G. A.; Lanzalunga, O.; Salamone, M. Time-Resolved Kinetic Study of the Electron-Transfer Reactions between Ring-Substituted Cumyloxyl Radicals and Alkylferrocenes. Evidence for an Inner-Sphere Mechanism. *J. Org. Chem.* **2011**, *76*, 1789−1794.

(8) Chatgilialoglu, C. (Me₃Si)₃SiH: Twenty Years After Its Discovery as a Radical-Based Reducing Agent. *Agent. Chem. Eur. J.* **2008**, *14*, 2310−2320.

(9) Lopinski, G. P.; Wayner, D. D. M.; Wolkow, R. A. Self-Directed Growth of Molecular Nanostructures on Silicon. *Nature* **2000**, *406*, 48−51.

(10) Kruse, P.; Johnson, E. R.; DiLabio, G. A.; Wolkow, R. A. Patterning of vinylferrocene on H-Si(100) via self-directed growth of molecular lines and STM-induced decomposition. *Nano Lett.* **2002**, *2*, 807−810.

(11) DiLabio, G. A.; Piva, P. G.; Kruse, P.; Wolkow, R. A. Dispersion Interactions Enable the Self-Directed Growth of Linear Alkane Nanostructures Covalently Bound to Silicon. *J. Am. Chem. Soc.* **2004**, *126*, 16048−16050.

(12) Clarkin, O. J. *Addition Reactions between Silicon Centered Radicals and Olefins: An Assessment of Theoretical Procedures.* M.Sc. Thesis, Carleton Univeristy, Ottawa, Canada, 2004.

(13) Chatgilialoglu, C.; Ingold, K. U.; Scaiano, J. C.; Woynar, H. Absolute Rate Constants for Some Reactions Involving Triethylsilyl Reactions in Solution. *J. Am. Chem. Soc.* **1981**, *103*, 3231−3232.

(14) Chatgilialoglu, C.; Ingold, K. U.; Scaiano, J. C. Absolute Rate Constants for the Addition of Triethylsilyl Radicals to Various Unsaturated Compounds. *J. Am. Chem. Soc.* **1983**, *105*, 3292−3296.

(15) Ballestri, M.; Chatgilialoglu, C.; Clark, K. B.; Griller, D.; Giese, B.; Kopping, B. Tris(trimethylsilyl)silane as a Radical-Based Reducing Agent in Synthesis. *J. Org. Chem.* **1991**, *56*, 678−683.

(16) Becke, A. D.; Johnson, E. R. Exchange-Hole Dipole Moment and the Dispersion Interaction Revisited. *J. Chem. Phys.* **2007**, *127*, 154108.

(17) Otero-de-la Roza, A.; Johnson, E. R. Non-Covalent Interactions and Thermochemistry using XDM-Corrected Hybrid and Range-Separated Hybrid Density Functionals. *J. Chem. Phys.* **2013**, *138*, 204109.

(18) Perdew, J. P.; Parr, R. G.; Levy, M.; Balduz, J. L. Density-Functional Theory for Fractional Particle Number — Derivative Discontinuities of the Energy. *Phys. Rev. Lett.* **1982**, *49*, 1691−1694.

(19) Zhang, Y.; W, Y. A Challenge for Density Functionals: Self-Interaction Error Increases for Systems with a Noninteger Number of Electrons. *J. Chem. Phys.* **1998**, *109*, 2604−2608.

(20) Yang, W.; Zhang, Y.; W, A. P. Degenerate Ground States and a Fractional Number of Electrons in Density and Reduced Density Matrix Functional Theory. *Phys. Rev. Lett.* **2000**, *84*, 5172−5175.

(21) Cohen, A. J.; Mori-Sanchez, P.; Yang, W. Insights into Current Limitations of Density Functional Theory. *Science* **2008**, *321*, 792−794.

(22) Cohen, A. J.; Mori-Sánchez, P.; Yang, W. Challenges for Density Functional Theory. *Chem. Rev.* **2011**, *112*, 289.

(23) Burke, K. Perspective on Density Functional Theory. *J. Chem. Phys.* **2012**, *136*, 150901.

(24) Becke, A. D. Perspective: Fifty Years of Density-Functional Theory in Chemical Physics. *J. Chem. Phys.* **2014**, *140*, 18A301.

(25) Tozer, D. J. Relationship between Long-Range Charge-Transfer Excitation Energy Error and Integer Discontinuity in Kohn−Sham Theory. *J. Chem. Phys.* **2003**, *119*, 12697−12699.

(26) Dreuw, A.; Weisman, J. L.; Head-Gordon, M. Long-Range Charge-Transfer Excited States in Time-Dependent Density Functional Theory Require Non-Local Exchange. *J. Chem. Phys.* **2003**, *119*, 2943−2946.

(27) Ruzsinszky, A.; Perdew, J. P.; Csonka, G. I.; Vydrov, O. A.; Scuseria, G. E. Spurious Fractional Charge on Dissociated Atoms: Pervasive and Resilient Self-Interaction Error of Common Density Functionals. *J. Chem. Phys.* **2006**, *125*, 194112.

(28) Cohen, A. J.; Mori-Sanchez, P.; Yang, W. Fractional Charge Perspective on the Band Gap in Density-Functional Theory. *Phys. Rev. B* **2008**, *77*, 115123.

(29) Sini, G.; Sears, J. S.; Bredas, J.-L. Evaluating the Performance of DFT Functionals in Assessing the Interaction Energy and Ground-State Charge Transfer of Donor/Acceptor Complexes: Tetrathiafulvalene-Tetracyanoquinodimethane (TTF-TCNQ) as a Model Case. *J. Chem. Theory Comput.* **2011**, *7*, 602−609.

(30) Janesko, B. G.; Scuseria, G. E. Hartree−Fock Orbitals Significantly Improve the Reaction Barrier Heights Predicted by Semilocal Density Functionals. *J. Chem. Phys.* **2008**, *128*, 244112.

(31) Zheng, X.; Liu, M.; Johnson, E. R.; Contreras-Garcia, J.; Yang, W. Delocalization Error of Density-Functional Approximations: A Distinct Manifestation in Hydrogen Molecular Chains. *J. Chem. Phys.* **2012**, *137*, 214106.

(32) Smith, J. M.; Alahmadi, Y. J.; Rowley, C. N. Range-Separated DFT Functionals Are Necessary to Model Thio-Michael Additions. *J. Chem. Theory Comput.* **2013**, *9*, 4860−4865.

(33) Johnson, E. R.; Salamone, M.; Bietti, M.; DiLabio, G. A. Modeling Noncovalent Radical-Molecule Interactions Using Conventional Density-Functional Theory: Beware Erroneous Charge Transfer. *J. Phys. Chem. A* **2013**, *117*, 947−952.

(34) Kim, M.-C.; Sim, E.; Burke, K. Understanding and Reducing Errors in Density Functional Calculations. *Phys. Rev. Lett.* **2013**, *111*, 073003.

(35) Johnson, E. R.; Otero-de-la Roza, A.; Dale, S. G. Extreme Density-Driven Delocalization Error for a Model Solvated-Electron System. *J. Chem. Phys.* **2013**, *139*, 184116.

(36) Becke, A. A. New Mixing of Hartree−Fock and Local Density-Functional Theories. *J. Chem. Phys.* **1993**, *98*, 1372.

(37) Lee, C.; Yang, W.; Parr, R. G. Development of the Colle−Salvetti Correlation-Energy Formula Into a Functional of the Electron Density. *Phys. Rev. B* **1988**, *37*, 785−789.

(38) Vydrov, O. A.; Scuseria, G. E. Assessment of a Long-Range Corrected Hybrid Functional. *J. Chem. Phys.* **2006**, *125*, 234109.

(39) Vydrov, O. A.; Heyd, J.; Krukau, A. V.; Scuseria, G. E. Importance of Short-Range Versus Long-Range Hartree−Fock Exchange for the Performance of Hybrid Density Functionals. *J. Chem. Phys.* **2006**, *125*, 074106.

(40) Otero-de-la Roza, A.; Johnson, E. R.; DiLabio, G. A. Halogen Bonding from Dispersion-Corrected Density-Functional Theory: The Role of Delocalization Error. *J. Chem. Theory Comput.* **2014**, *10*, 5436−5447.

(41) Johnson, E. R.; Clarkin, O. J.; DiLabio, G. A. Density Functional Theory Based Model Calculations for Accurate Bond Dissociation Enthalpies. 3. A Single Approach for XH, XX, and XY (X, Y = C, N, O, S, Halogen) Bonds. *J. Phys. Chem. A* **2003**, *107*, 9953−9963.

(42) Johnson, E. R.; Otero-de-la Roza, A.; Dale, S. G.; DiLabio, G. A. Efficient Basis Sets for Non-Covalent Interactions in XDM-Corrected Density-Functional Theory. *J. Chem. Phys.* **2013**, *139*, 214109.

(43) Jensen, F. Polarization Consistent Basis Sets. II. Estimating the Kohn−Sham Basis Set Limit. *J. Chem. Phys.* **2002**, *116*, 7372−7379.

(44) Jensen, F.; Helgaker, T. Polarization Consistent Basis Sets. V. The Elements Si−Cl. *J. Chem. Phys.* **2004**, *121*, 3463−3470.

(45) Fischer, H.; Radom, L. Factors Controlling the Addition of Carbon-Centered Radicals to Alkenes: An Experimental and Theoretical Perspective. *Angew. Chem., Int. Ed.* **2001**, *40*, 1340−1371.

(46) Loh, S. K.; Beach, D. B.; Jasinski, J. M. Absolute Rate Constants for the Reaction of Silyl with Nitric-Oxide, Ethylene, Propyne, and Propylene, and the Silyl Recombination Reaction. *Chem. Phys. Lett.* **1990**, *169*, 55−63.

(47) Arthur, N. L.; Potzinger, P. The $H/(CH_3)_3SiH/C_2H_4$ Reaction System and the Addition of $(CH_3)_3Si$ to Ethene. An End-Product Study. *Organometallics* **2002**, *21*, 2874−2890.

(48) Frisch, M. J.; et al. *Gaussian 09*, revision A.1; Gaussian Inc.: Wallingford, CT, 2009.

(49) Scalmani, G.; Frisch, M. J. Continuous Surface Charge Polarizable Continuum Models of Solvation. I. General Formalism. *J. Chem. Phys.* **2010**, *132*, 114110.

(50) Koerzdoerfer, T.; Sears, J. S.; Sutton, C.; Bredas, J. L. Long-Range Corrected Hybrid Functionals for π-Conjugated Systems: Dependence of the Range-Separation Parameter on Conjugation Length. *J. Chem. Phys.* **2011**, *135*, 204107.